J. Electrochem. Sci. Eng. **12(5)** (2022) 901-909; https://dx.doi.org/10.5599/jese.1319

Open Access : : ISSN 1847-9286
https://pub.iapchem.org/ojs/index.php/JESE

Original scientific paper

Effect of nano yttria-stabilized zirconia on properties of Ni-20Cr composite coatings

Sukhjinder Singh[1,✉], Khushdeep Goyal[1] and Rakesh Bhatia[2]

[1]*Department of Mechanical Engineering, Punjabi University, Patiala, India*
[2]*Yadavindra Department of Engineering, Punjabi University Guru Kashi Campus, Damdama Sahib, India*

Corresponding author: ✉*sukhjindermoga@gmail.com ; Tel.: +91-9876785500*

Received: March 4, 2022; Accepted: July 18, 2022; Published: August 16, 2022

Abstract

In the present work, 5 and 10 wt.% yttria-stabilized zirconia (YSZ) nanoparticles were reinforced in Ni-20Cr powder and deposited on boiler tube steel using a high-velocity oxy-fuel spraying process. The effect of YSZ reinforcement on microhardness, surface roughness and porosity were investigated. The hardness was the highest for nanocomposite coating reinforced with 10 wt.% YSZ and hardness was found to increase with a decrease in porosity. The coating microstructure and elements were characterized using field emission scanning electron microscopy (FE-SEM) with an energy dispersive spectroscope (EDS). The constituents of the coating were identified using X-ray diffractometer. It was found that the composite coating with 10 wt.% YSZ reinforced nanocomposite coating has the highest microhardness, in the range of 1008-1055 hv. During the coating process, nano YSZ particles were dispersed in the gaps between the micrometric Ni-20Cr particles, providing a better coating matrix than conventional Ni-20Cr. The Ni-20Cr with 10 wt.% of YSZ nanoparticles showed better results in terms of mechanical and microstructural properties during the investigation.

Keywords

Thermal spray coatings; nanocomposites; porosity, hardness, microstructure; oxy-fuel; HVOF

Introduction

The desire to raise the power output of thermal power plants is the main drive for the inventions of novel materials due to increasing market competition. Heat and corrosion-resistant coatings are among the novel materials used in these units [1,2]. The coatings are applied to the surface of boiler steels used in thermal plants in order to slow down their deterioration [2-4]. Surface modifications of these components result from corrosion and erosion in a high-temperature environment. Surface changes result in a loss of quality, which eventually leads to sudden premature failure [2,3]. The thermal spray coatings extend the life of these boiler steels in high-temperature environments significantly [4].

Various thermal spraying techniques, such as flame spraying, plasma spraying, arc spraying, and high-velocity oxygen fuel (HVOF) techniques, are used to coat the components of these power

plants. Due to the powder spraying technique, these coatings have a large number of pores, and corroding species attack the substrate steels through these pores [4-6]. With the development of an oxide layer, this attack induces alterations in the microstructure. The failure of thermal spray coatings has been linked to the severe development of oxide layers [7]. Many researchers have discovered that changing the microstructure of these coatings can increase their corrosion resistance [8,9]. The microstructure of coatings is affected by various coating spraying procedures, as well as post-treatment of as-sprayed coatings [10]. Using composing powders, some researchers have altered the microstructure of coatings. Traditional powders were combined with nano-size ceramic powders, cermet, and rare earth oxides to create composite coatings. Because of the possibilities of synthesizing a surface protection layer with unique physical-chemical properties often not achieved in conventional materials, nanostructured coatings composed of crystalline/amorphous nanophase mixtures have recently gained interest in developing corrosion resistance coatings [11]. Nanostructured materials are a new type of engineering material with improved characteristics and a structural length scale ranging from 1 to 100 nm [12]. Shaw *et al*. [13] investigated the relationship between microstructure and nanostructure properties, as well as those of nanostructured coatings and plasma spray settings. Using reconstituted nanosized Al_2O_3 and TiO_2 powder, plasma spray was used to create Al_2O_3 – 13 wt.% TiO_2 coatings [14]. Mohsen *et al*. [10] and Saremi *et al*. [15] combined YSZ powder with alumina to create a composite coating that reduced the thickness of the oxide layer and improved corrosion resistance at high temperatures. Yugeswaran *et al*. [16] revealed that a number of interfaces are higher in composite coatings than in conventional coatings, which causes blocking of the micro-pores. This blocking causes a hindrance to the corrosion species and improves corrosion resistance.

Many authors have reported the development of Ni-20Cr coatings on steel alloys [17-23], but no researcher has deposited nano yttria-stabilized zirconia (Y_2O_3/ZrO_2) (YSZ) reinforced composite coatings on boiler steels. Therefore, there is a scope to develop new nano yttria-stabilized zirconia (YSZ) reinforced (Ni-20Cr) nanocomposite coatings and subsequently deposit and investigate the microstructure, porosity, and microhardness of these newly developed composite coatings on boiler tube steel.

In this research work, HVOF sprayed 5 and 10-weight percent YSZ-(Ni-20Cr) nanocoatings were developed and deposited on T22 boiler tube steel. The microstructure, porosity and microhardness of these newly developed composite coatings have been investigated. HVOF thermal spraying technique was used in this research work because the coatings produced with the HVOF method have high adhesive strength with the base material and also individual splats have high cohesive strength [24,25]. Goyal *et al.* [26] have observed that this spraying process provides homogeneous coatings having a low value of porosity along with high hardness.

Experimental

Coating material

To generate different coating powders, commercially available Ni-20Cr powder was blended with 5 and 10 wt.% YSZ powder using low energy ball milling. 950 Ni-20Cr powder was mixed with 50 g YSZ (Y_2O_3/ ZrO_2) powder to get the composite mixture. Similarly, 900 g Ni-20Cr powder was mixed with 10 g YSZ (Y_2O_3/ ZrO_2) powder. The composite powders were continuously rolled for four hours at a speed of 200 rpm.

The T22 steel substrates were cut from the boiler tubes procured from Guru Gobind Singh Thermal Power Plant, Ropar, India. The sample size was 22×15×5 mm. The T22 substrates were polished with SiC paper, and subsequently, grit was blasted with alumina powder of grit 45. The substrates were coated using high-velocity oxy-fuel spraying equipment at Metallizing Equipment Co. Pvt. Ltd. Jodhpur, India. The process parameters of the HVOF spraying method are shown in Table 1. During the spraying procedure, these process parameters were kept constant.

Table 1. *HVOF spraying process parameters*

Oxygen flow rate, L min^{-1}	260
Fuel (Acetylene) flow rate, L min^{-1}	80
Air-flow rate, L min^{-1}	560
Spray distance, mm	220
Powder feed rate, g min^{-1}	25
Fuel pressure, kg cm^{-2}	1.4
Oxygen pressure, kg cm^{-2}	2.40
Air pressure, kg cm^{-2}	3.50

Mechanical properties, microstructural properties and phase characterization of coatings

Using a Minitest-2000 thin film thickness gauge, the coating thickness was measured during the thermal spraying process. To expose the coating cross-section, the coated samples were sectioned, mounted in epoxy, and polished. With a load of 300 g, the microhardness of the coating was tested along the coating cross-section with a Vickers hardness tester. The surface roughness of the uncoated and coated samples was measured with the help of a surface roughness tester (Surftest SJ310, Mitutoyo). From SEM micrographs of the cross-section, the porosity of the HVOF sprayed Ni-20Cr, 5 and 10 wt.% YSZ reinforced Ni-20Cr nanocomposite coatings were assessed using an image analysis method employing LEICA Image analyzer software. The pore area size is calculated using a computer-based porosity analysis technique that converts grey-level areas (pore areas) into a background different from the rest of the microstructure. After that, the computer system counts the number of pixels. The average of five porosity measurements was calculated for each type of coated specimen. FE-SEM was used to examine the microstructure of Ni-20Cr, 5 and 10 wt.% YSZ reinforced Ni-20Cr nanocomposite coatings. Using an X-ray diffractometer, the phases in the conventional and CNT-enhanced coatings were discovered. To investigate the various phases, present in all types of samples, XRD analysis was carried out using PANalytical X'Pert Pro x-ray diffractometer with the copper target (0.15419, 40 kV and 45 mA). Phase identification was made with High Score PLUS software.

Results and discussion

The thickness, porosity, surface roughness and microhardness values of Ni-20Cr, 5 and 10 wt.% YSZ reinforced Ni-20Cr nanocomposite coatings are shown in Table 2.

Table 2. *Average coating thickness, porosity and surface roughness values for different coatings*

Substrate	Coating type	Coating thickness, µm	Porosity, %	Average surface roughness, µm
ASME-SA213-T22	Ni-20Cr	252	1.89	3.98
	5 wt.% YSZ- (Ni-20Cr)	255	1.67	3.32
	10 wt.% YSZ- (Ni-20Cr)	253	1.38	2.86

The average coating thickness for all the coatings was in the range of 250-255 µm. The average thickness of Ni-20Cr was measured as 255 µm, whereas the average thicknesses of 5 and 10 wt.% YSZ reinforced Ni-20Cr nanocomposite coatings were 255 and 253 µm. The thermal spray coating is usually porous in nature, which affects coatings' properties. The porosity values of Ni-20Cr and YSZ reinforced Ni-20Cr nanocomposite coatings were less than 2 %. The Ni-20Cr coating showed a porosity value of 1.89 %. The porosity value of 5 wt.% YSZ- (Ni-20Cr) was found to be 1.67 %. The composite coating with 10 wt.% YSZ was found to be denser with 1.38 % porosity. With the addition of nano yttria-stabilized zirconia (Y_2O_3/ZrO_2), the porosity of nanocomposite coatings was significantly reduced. The surface roughness values for Ni-20Cr conventional coating, 5 wt.% YSZ- (Ni-20Cr) and 10 wt.% YSZ- (Ni-20Cr) nanocomposite coated samples were found to be 3.98, 3.32 and 2.86, respectively. Better surface characteristics were observed for 10 wt.% YSZ- (Ni-20Cr) nanocomposite coating as compared to conventional Ni-20Cr coating as the surface roughness was decreased by the addition of YSZ nanoparticles. The lower value of the porosity for 5 wt.% YSZ- (Ni-20Cr) nanocomposite coating is the main reason for the reduction in surface roughness.

The higher degree of melting of nanoparticles reinforced powders causes a decrease in porosity with increasing nanoparticle concentration [24,25]. The nano yttria-stabilized zirconia distributed in the Ni-20Cr matrix can absorb more heat, resulting in improved powder particle melting. According to Goyal *et al.* [25], accelerated melting is caused by the higher thermal conductivity of nanoparticles. The inflight temperature is affected by nanoparticle content and uniform distribution, which further affects heat transfer and results in a dense composite coating [25,26].

Figure 1 shows the microhardness profiles for Ni-20Cr conventional coating, 5 wt.% YSZ- (Ni-20Cr) and 10 wt.% YSZ- (Ni-20Cr) nanocomposite coatings. The hardnesses of Ni-20Cr conventional coating, 5 wt.% YSZ- (Ni-20Cr) and 10 wt.% YSZ- (Ni-20Cr) nanocomposite coated specimens were found to be in the range of 712-759 Hv, 912-964 Hv, and 1008-1055 Hv, respectively. The hardness values of nanocomposite coatings increased with an increase in nano yttria-stabilized zirconia content in the coating. The nano yttria-stabilized zirconia particles were able to increase the hardness values of the composite Ni-20Cr coatings.

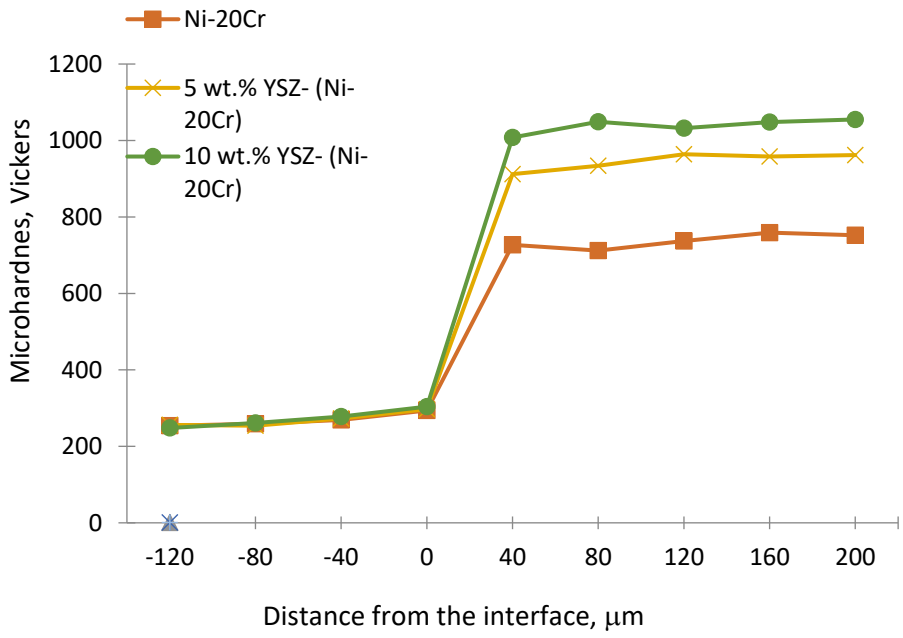

***Figure 1**. Microhardness profiles of Ni-20Cr conventional coating across the cross-section*

The hardnesses of Ni-20Cr conventional coating, 5 wt.% YSZ- (Ni-20Cr) and 10 wt.% YSZ- (Ni-20Cr) nanocomposite coated specimens were found to be in the range of 712-759, 912-964 and 1008-1055 Hv, respectively. The hardness values of nanocomposite coatings increased with an increase in nano yttria-stabilized zirconia content in the coating. The nano yttria-stabilized zirconia particles were able to increase the hardness values of the composite Ni-20Cr coatings. The nano yttria-stabilized zirconia particles were able to fill the pores in the Ni-20Cr matrix and reduced the porosity of the coating, which caused an increase in hardness. The microhardness profiles clearly show that the hardness through the coating cross-section was found to be nearly uniform for all coated specimens.

The increase in hardness has been attributed by Porthina *et al.* [27] and Kumar *et al.* [28] to the decrease in porosity. Due to the closure of porosities, the inclusion of YSZ nanoparticles increased the resistance to indentation. Due to accelerated melting, nano YSZ particles were able to fill the spaces between the Ni-20Cr particles, resulting in an increase in the hardness of composite coatings as YSZ concentration increased. Increased hardness of YSZ reinforced composites is attributed to fracture suppression and improved dispersion hardening [29]. The effect of carbon-based nano-particle reinforcement has been firmly substantiated by the increase in hardness of composite coatings, as described in the literature [30-32].

The X-ray diffraction spectra for all coatings are shown in Figure 2.

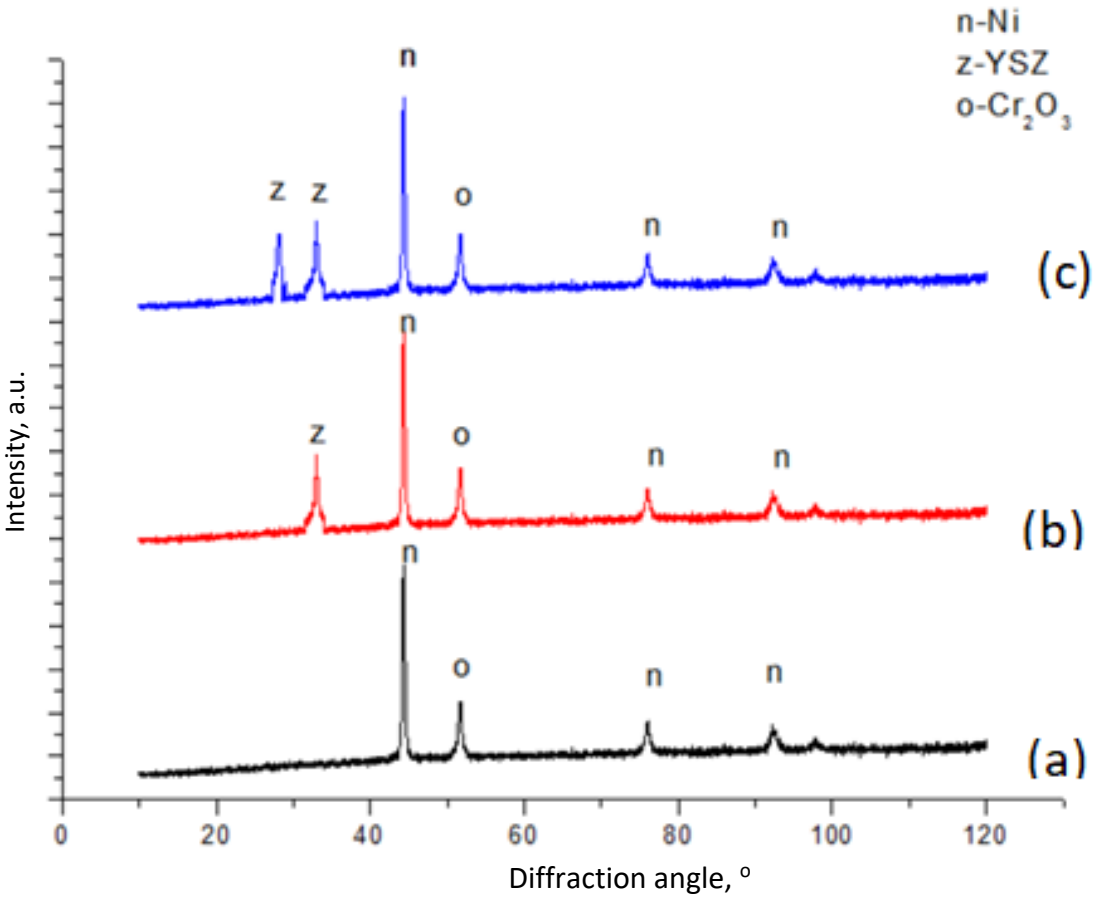

Figure 2. *XRD profiles of HVOF sprayed coatings: (a) Ni-20Cr; (b) 5 wt.% YSZ- (Ni-20Cr); (c) 10 wt.% YSZ- (Ni-20Cr)*

XRD profile of Ni-20Cr coated T22 boiler tube steel sample shows Ni as the main phase, along with traces of Cr. The XRD profile of the Ni-20Cr coating reinforced with 5 and 10 wt.% YSZ nanoparticles revealed that chromium and carbon are present as a major phase, and the presence

of nickel, yttrium, and zirconium was also observed as a minor phase. The identical phases were obtained for all coatings. Because of the rapid cooling during the spraying process, the development of non-crystalline amorphous phases increases in cases of YSZ reinforced nanocomposite coatings. The XRD patterns depicted that the HVOF method can effectively limit the generation of decarburization phases because of the high velocity and relatively low temperature of the flame.

Figure 3 shows FE-SEM micrographs obtained with energy dispersive X-Ray spectroscopy analysis for HVOF sprayed Ni-20Cr nanocomposite coatings on T22 boiler steel, as well as 5 and 10 wt.% YSZ reinforced Ni-20Cr nanocomposite coatings.

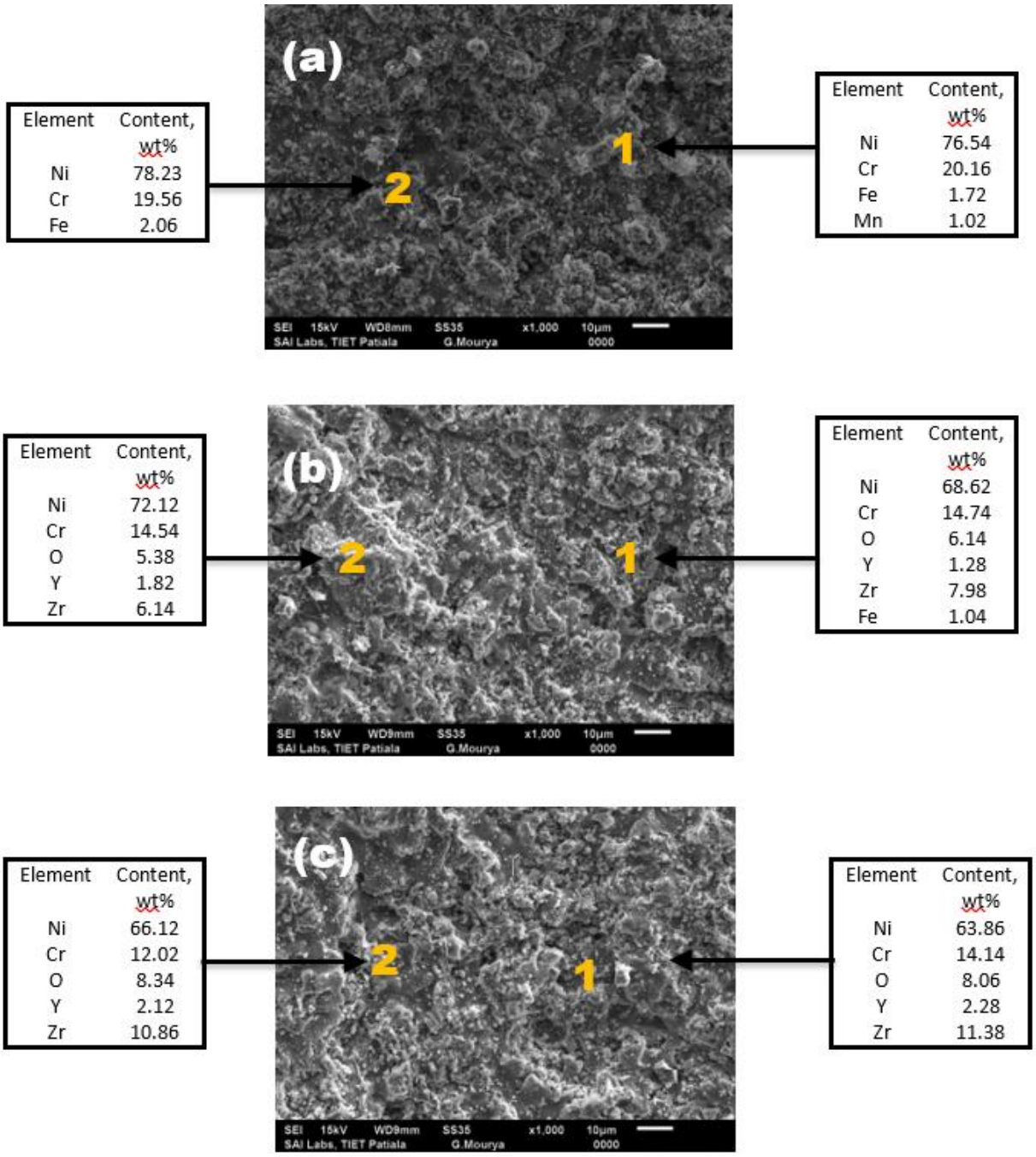

***Figure 3**. FE-SEM with energy dispersive spectroscopy analysis of HVOF sprayed coatings: (a) Ni-20Cr; (b) 5 wt.% YSZ- (Ni-20Cr); (c) 10 wt.% YSZ- (Ni-20Cr)*

As illustrated in Figure 3a, the microstructure of Ni-20Cr coating is dense, consisting of interlocking particles of regular shape. Several oxide stringers may also be seen in the coating

microstructure. As illustrated in Figures 3b and 3c, the YSZ nanoparticles diffused uniformly in the Ni-20Cr matrix. The use of YSZ nanoparticles to strengthen the coating layer resulted in a dense and uniform layer. The microstructures demonstrate that in the composite coating, homogeneous coalescence of nano YSZ has happened with the base Ni-20Cr matrix. Energy dispersive spectroscopy analysis revealed that the elemental composition of the various coatings was comparable to that of the feedstock powder, as shown in Figure 3. The presence of Fe and Mn in the Ni-20Cr conventional coating was found by EDS analysis, which could be attributable to Fe and Mn migration from the substrate to the coating matrix due to porosity in conventional coating. Diffusion of base elements through pores/voids in the coating matrix has also been reported by various authors [32-35]. Reinforcement of nano YSZ particles in Cr3C2-25NiCr coating filled the gaps, reducing porosity which prevents diffusion of base elements to the coating matrix, thereby increasing the microhardness of the coatings.

Conclusions

The following conclusions are made from this experimental work:

- The thicknesses of HVOF sprayed Ni-20Cr, 5 and 10 wt.% YSZ reinforced Ni-20Cr nanocomposite coatings were determined to be between 250 and 255 μm.
- As the amount of YSZ in a nanocomposite coating increases, the porosity value lowers. The 1.38 % porosity of the 10 wt.% YSZ-(Ni-20Cr) coating was revealed to be the lowest. The surface roughness values are improved as the porosity decreases.
- The composite coating with 10 wt.% YSZ reinforced nanocomposite coating showed the highest microhardness, which was in the range of 1008-1055 Vickers. This could be due to nano YSZ particles filling pores/voids in the coating matrix.
- The quick cooling of the spraying procedure resulted in the formation of non-crystalline amorphous phases, as evidenced by the XRD spectra of all nanocomposite coatings.
- The presence of Fe and Mn in the Ni-20Cr coating was detected by SEM/EDS analysis, which could be attributed to the diffusion of these elements through holes in the coating matrix. SEM/EDS investigation of YSZ reinforced nanocomposite coatings revealed a homogeneous, dense coating surface with no base element diffusion due to nanoparticle filling of voids/pores.

Acknowledgement and conflict of interest statement: *This research received no specific grant from any funding agency in the public, commercial, or not-for-profit sectors. The authors also declare that they have no conflict of interest.*

References

[1] C. A. Duarte, E. Espejo, J. C. Martinez, *Engineering Failure Analysis* **79** (2017) 704-713. https://doi.org/10.1016/j.engfailanal.2017.05.032

[2] Q. Ding, X.-F. Tang, Z.-G. Yang, *Engineering Failure Analysis* **73** (2017) 129-138. https://doi.org/10.1016/j.engfailanal.2016.12.011

[3] M. Loghman-Estarki, R. S. Razavi, H. Edris, S. Bakhshi, M. Nejati, H. Jamali, *Ceramics International* **42(6)** (2016) 7432-7439. https://doi.org/10.1016/j.ceramint.2016.01.147

[4] Goyal, H. Singh, R. Bhatia, *International Journal of Minerals, Metallurgy and Materials* **26** (2019) 337-344. https://doi.org/10.1007/s12613-019-1742-8

[5] V. Pal Singh, K. Goyal, R. Goyal. *Australian Journal of Mechanical Engineering* **17(2)** (2019) 127-132. https://doi.org/10.1080/14484846.2017.1364834

[6] S. Saladi, J. Menghani, S. Prakash, *Transactions of the Indian Institute of Metals* **67(5)** (2014) 623-627. https://doi.org/10.1007/s12666-014-0383-x

[7] V. P. Singh Sidhu, K. Goyal, R. Goyal, *Advanced Engineering Forum* **20** (2017) 1-9. https://doi.org/10.4028/www.scientific.net/AEF.20.1
[8] P. Bengtsson, T. Johannesson, *Journal of Thermal Spray Technology* **4(3)** (1995) 245-251. https://doi.org/10.1007/BF02646967
[9] A. Singh, K. Goyal, R. Goyal, B. Krishan, *Journal of Bio-and Tribo-Corrosion* **7(1)** (2021) 21. https://doi.org/10.1007/s40735-020-00461-9
[10] C. J. Li, G. J. Yang, C. X. Li, *Journal of Thermal Spray Technology* **22(2)** (2013) 192-206. https://doi.org/10.1007/s11666-012-9864-9
[11] J. A. Gan, C. C. Berndt, *International Materials Reviews* **60(4)** (2015) 195-244. https://doi.org/10.1179/1743280414Y.0000000048
[12] K. Bobzin, F. Ernst, J. Zwick, T. Schlaefer, D. Cook, K. Nassenstein, A. Schwenk, *Journal of Thermal Spray Technology* **17(3)** (2008) 344-351. https://doi.org/10.1007/s11666-008-9188-y
[13] L. L. Shaw, D. Goberman, R. Ren, M. Gell, S. Jiang, Y. Wang, T. D. Xiao, P. R. Strutt, *Surface and Coatings Technology* **130(1)** (2000) 1-8. https://doi.org/10.1016/S0257-8972(00)00673-3
[14] D. Goberman, Y. H. Sohn, L. Shaw, E. Jordan, M. Gell, *Acta Materialia* **50(5)** (2002) 1141-1152. https://doi.org/10.1016/S1359-6454(01)00414-1
[15] M. Saremi, A. Afrasiabi, A. Kobayashi, *Surface and Coatings Technology* **202(14)** (2008) 3233-3238. https://doi.org/10.1016/j.surfcoat.2007.11.029
[16] S. Yugeswaran, C. Yoganand, A. Kobayashi, K. Paraskevopoulos, B. Subramanian, *Journal of the Mechanical Behavior of Biomedical Materials* **9** (2012) 22-33. https://doi.org/10.1016/j.jmbbm.2011.11.002
[17] S Singh, K Goyal, R Goyal, *Chemical and Materials Engineering* **4(4**) (2016) 57-64. https://doi.org/10.13189/cme.2016.040401
[18] A. Kumar, V. Srivastava, N. K. Mishra, *IOP Conference Series: Materials Science and Engineering* **377** (2018) 012076. https://doi.org/10.1088/1757-899X/377/1/012076
[19] M. Kumar, S. Kant, S. Kumar, *Materials Research Express* **6** (2019) 106427. https://doi.org/10.1088/2053-1591/ab3bd8
[20] S. Kumar, M. Kumar, A. Handa, *Materials at High Temperatures* **37(6**) (2020) 370-384. https://doi.org/10.1080/09603409.2020.1810922
[21] W. Tillmann, D. Kokalj, D. Stangier, V. Schöppner, H. Malatyali, *Sensors* **19(15)** (2019) 3414. https://doi.org/10.3390/s19153414
[22] W. Zhang, C. Wang, Q. Song, H. Cui, X. Feng, C. Zhang, *Metallurgical and Materials Transactions A* **50(11)** (2019) 5410-5420. https://doi.org/10.1007/s11661-019-05440-5
[23] R. Kumar, R. Kumar, S. Kumar, *International Journal of Science and Management Studies* (IJSMS) **1(3)** (2018) 1-6. https://doi.org/10.51386/25815946/ijsms-v1i3p101
[24] K. Goyal, *Tribology-Materials, Surfaces & Interfaces* **12(2)** (2018) 97-106. https://doi.org/10.1080/17515831.2018.1452369
[25] K. Goyal, H. Singh, R. Bhatia, *Advanced Engineering Forum* **26** (2018) 53-66. https://doi.org/10.4028/www.scientific.net/AEF.26.53
[26] K. Goyal, *World Journal of Engineering* **16(1)** (2019) 64-70. https://doi.org/10.1108/WJE-08-2018-0262
[27] A. Portinha, V. Teixeira, J. Carneiro, J. Martins, M. Costa, R. Vassen, D. Stoever, *Surface and Coatings Technology* **195(2-3)** (2005) 245-251. https://doi.org/10.1016/j.surfcoat.2004.07.094
[28] R. Kumar, D. Bhandari, K. Goyal, *Journal of Electrochemical Science and Engineering* **12(4)** (2022) 651-666. https://doi.org/10.5599/jese.1190

[29] S. V. Bhaskar, T. Rajmohan, K. Palanikumar, B. B. G. Kumar, *Journal of the Institution of Engineers (India): Series D* **97(1)** (2016) 59-67. https://doi.org/10.1007/s40033-015-0074-8
[30] P. R. Silva, V. O. Almeida, G. B. Machado, E. V. Benvenutti, T. M. H. Costa, M. R. Gallas, *Langmuir* **28(2)** (2011) 1447-1452. https://doi.org/10.1021/la203056f
[31] K. Goyal, H. Singh, R. Bhatia, *International Journal of Minerals, Metallurgy and Materials* **26** (2019) 337-344. https://doi.org/10.1007/s12613-019-1742-8
[32] K. Balani, T. Zhang, A. Karakoti, W. Li, S. Seal, A. Agarwal, *Acta Materialia* **56(3)** (2008) 571-579. https://doi.org/10.1016/j.actamat.2007.10.038
[33] D.-S. Lim, D.-H. You, H.-J. Choi, S.-H. Lim, H. Jang, *Wear* **259(1-6)** (2005) 539-544. https://doi.org/10.1016/j.wear.2005.02.031
[34] K. Goyal, R. Goyal, *Surface Engineering* **36(11)** (2020) 1200-1209. https://doi.org/10.1080/02670844.2019.1662645
[35] K. Goyal, H. Singh, R. Bhatia, *Journal of the Australian Ceramic Society* **55** (2019) 315- 322. https://doi.org/10.1007/s41779-018-0237-9